Chronic kidney disease aggravates arteriovenous fistula damage in rats

Stephan Langer[1], Maria Kokozidou[1], Christian Heiss[2], Jennifer Kranz[1], Tina Kessler[1], Niklas Paulus[1], Thilo Krüger[3], Michael J. Jacobs[1,4], Christina Lente[5] and Thomas A. Koeppel[1]

[1]European Vascular Center Aachen-Maastricht, Department of Vascular Surgery, University Hospital RWTH Aachen, Aachen, Germany; [2]Division of Cardiology, Pulmonology and Vascular Medicine, Department of Medicine B, Heinrich-Heine University Düsseldorf, Düsseldorf, Germany; [3]Division of Nephrology and Clinical Immunology, University Hospital RWTH Aachen, Aachen, Germany; [4]European Vascular Center Aachen-Maastricht, Department of Vascular Surgery, University Hospital Maastricht, Maastricht, The Netherlands and [5]Department of Medical Statistics, University Hospital RWTH Aachen, Aachen, Germany

Neointimal hyperplasia (NIH) and impaired dilatation are important contributors to arteriovenous fistula (AVF) failure. It is unclear whether chronic kidney disease (CKD) itself causes adverse remodeling in arterialized veins. Here we determined if CKD specifically triggers adverse effects on vascular remodeling and assessed whether these changes affect the function of AVFs. For this purpose, we used rats on a normal diet or on an adenine-rich diet to induce CKD and created a fistula between the right femoral artery and vein. Fistula maturation was followed noninvasively by high-resolution ultrasound (US), and groups of rats were killed on 42 and 84 days after surgery for histological and immunohistochemical analyses of the AVFs and contralateral femoral vessels. *In vivo* US and *ex vivo* morphometric analyses confirmed a significant increase in NIH in the AVFs of both groups with CKD compared to those receiving a normal diet. Furthermore, we found using histological evaluation of the fistula veins in the rats with CKD that the media shrank and their calcification increased significantly. Afferent artery dilatation was significantly impaired in CKD and the downstream fistula vein had delayed dilation after surgery. These changes were accompanied by significantly increased peak systolic velocity at the site of the anastomosis, implying stenosis. Thus, CKD triggers adverse effects on vascular remodeling in AVFs, all of which contribute to anatomical and/or functional stenosis.

Kidney International advance online publication, 29 September 2010; doi:10.1038/ki.2010.353

KEYWORDS: arteriovenous fistula; arteriovenous shunt; chronic kidney disease; dialysis access; vascular access

Correspondence: *Stephan Langer, European Vascular Center Aachen-Maastricht, Department of Vascular Surgery, University Hospital Aachen, Pauwelsstrasse 30, Aachen 52074, Germany.*
E-mail: slanger@ukaachen.de

Received 3 February 2010; revised 7 May 2010; accepted 9 June 2010

Arteriovenous fistula (AVF) surgery is widely accepted as the method of choice for dialysis access in patients with end-stage renal disease.[1] However, the 1-year patency rates of AVFs are estimated to be only 63%,[2] and recurrent AVF failure is a major cause for morbidity and mortality of those patients. The inability of the vein to dilate might cause maturation failure in the early postoperative course.[3] Moreover, neointimal hyperplasia (NIH) may result in stenosis and, ultimately, occlusion.[4] Morphologically, NIH results from proliferation of smooth muscle cells (SMCs) combined with matrix deposition.

Chronic kidney disease (CKD) is associated with vascular damage, and it is likely that uremia may impair AVF patency too. Calcification of arteries due to media-sclerosis is a well-known phenomenon in dialysis patients.[5] Even though vascular access calcification is also commonly observed in hemodialysis patients,[6] it is not known whether this may affect fistula function.

Assessing how CKD specifically affects fistula failure in humans is problematic, because AVF surgery is almost exclusively performed in patients with end-stage renal disease. In this context, small animal AVF models have attracted great attention. The functional, structural, and molecular responses in fistula veins following arterialization have been recently described in mice[7] and rats.[8–11] The majority of these experiments, however, was performed in animals without CKD. In a very recent study, it was demonstrated that CKD accelerates the development of NIH due to increased vascular SMC migration.[12]

However, phenotypical analysis of NIH cell composition was not performed and it remained unclear whether these specific changes affected fistula hemodynamics. Consequently, the aim of the current study was to identify whether CKD specifically triggers adverse effects on vascular remodeling and to assess whether these changes are of functional relevance.

RESULTS

Surgical procedure

AVF surgery was successful in all rats (group no. 1 = normal diet, group no.2 = CKD) without any procedure-related complications. The mean surgical time was 32 min (range: 26–41). All animals survived the surgery, but two rats of group no. 1 died between days 21 and 42 after surgery for unknown reasons. The patency rate of the AVFs was 96% at the time of harvesting. During the observation period, there were no signs of peripheral ischemia resulting from steal or edema caused by venous congestion.

Table 1 | Serum creatinine, serum calcium, serum phosphate and serum albumin levels of rats fed with an adenine-rich diet

Constituent	Feeding period (days)	Adenine diet	*P*-value (difference to baseline)
Creatinine, μmol/l	−21 (baseline)	33.17 ± 2.91	
	0 (surgery)	80.50 ± 50.28	0.054
	21	63.75 ± 18.62	0.008
	42	58.50 ± 12.26	0.003
	63	91.75 ± 22.40	0.001
	84	48.50 ± 5.85	0.001
Calcium, mmol/l	−21 (baseline)	2.71 ± 0.09	
	0 (surgery)	2.67 ± 0.20	0.692
	21	2.48 ± 0.06	0.004
	42	2.72 ± 0.07	0.838
	63	2.81 ± 0.13	0.233
	84	2.49 ± 0.36	0.230
Phosphorous, mmol/l	−21 (baseline)	1.71 ± 0.46	
	0 (surgery)	2.27 ± 0.75	0.167
	21	1.52 ± 0.26	0.530
	42	2.91 ± 0.25	0.003
	63	1.71 ± 0.19	0.913
	84	1.75 ± 0.48	0.021
Albumin, g/l	−21 (baseline)	41.67 ± 3.78	
	0 (surgery)	32.00 ± 3.00	0.001
	21	28.25 ± 2.86	0.001
	42	26.75 ± 3.27	0.001
	63	32.50 ± 0.50	0.003
	84	30.00 ± 0.71	0.001

Values are mean ± s.d.

Blood biochemistry and systolic blood pressure

As shown in Table 1, CKD was established 3 weeks after feeding an adenine-rich diet to the rats of group no. 2. At the time of surgery, serum creatinine values were 2.4 times those of the baseline values. Subsequently, the creatinine values remained significantly elevated throughout the study period. Serum albumin and serum calcium were decreased by 23 and 1.5 % at the time of surgery and by 28 and 8% at the end of the study period. Immediately before surgery, the serum phosphate levels were increased by 25% and by 48% on day 42 after surgery. On day 84 after surgery, only a moderate effect on the phosphate level was verifiable. The mean systolic blood pressure was 116.2 ± 11.2 mm Hg at baseline. After a 3-week feeding period, healthy animals of group no. 1 and CKD rats of group no. 2 exhibited no significant difference in systolic blood pressure (127.7 ± 11.8 mm Hg vs 130.5 ± 18.5 mm Hg; $P > 0.05$).

Sono-morphological and functional characterization of AVF maturation

The *in vivo* ultrasound (US) examinations confirmed progressive NIH. Figure 1 shows a representative duplex-US image of neighboring femoral artery and AVF as well as respective B-Mode images containing pulse-waved Doppler flow velocity tracings. The evolution of the NIH is depicted in Figure 2a. Pronounced thickening of the neointimal complex was observed in the fistula veins of all animals. The neointima of group no. 1 animals showed a moderate increase within the first 3 weeks after surgery (baseline: 0.033 ± 0.006 mm; day 21: 0.140 ± 0.017 mm, $P = 0.001$) and a plateau thereafter until day 84 (0.150 ± 0.032 mm, $P = 0.012$ vs baseline value). In contrast, the CKD rats developed progressively more neointimal thickening, which plateaued only after day 63 (baseline: 0.087 ± 0.029 mm; day

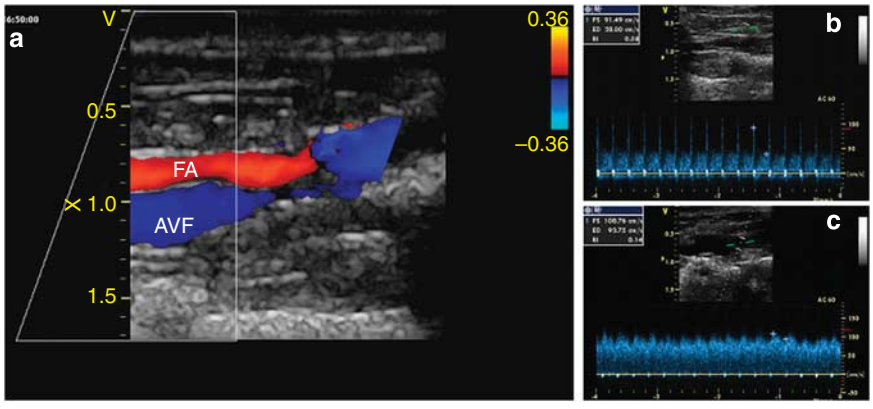

Figure 1 | Ultrasound of the arterialized vein. Representative duplex-ultrasound image (**a**) of the femoral artery (FA) and the arteriovenous fistula (AVF) in a rat of group no. 1 on day 84 after surgery. Shown on the right side is B-Mode images combined with Doppler flow velocity tracings of the (**b**) afferent artery and (**c**) AVF. Horizontal marks on the scale bar represent the depth of ultrasound impression (cm) and the velocities (cm/s).

63: 0.340 ± 0.030 mm, $P = 0.001$ vs baseline value; day 84: 0.350 ± 0.030 mm, $P = 0.002$ vs day 84 group no. 1).

Parallel to NIH development, there were also changes observed in the vessel diameter after AVF surgery in healthy and uremic animals. In healthy animals (group no. 1), both the afferent artery and AVF vein exhibited significant dilation during the first 3 and 2 weeks, respectively. Thereafter, vessel dilation remained constant at 176 and 220% of baseline values, respectively. In CKD animals, this response was impaired with veins only dilating to 142% of their original size and femoral arteries exhibiting a significant contraction to 80% of their original size (Figure 2b).

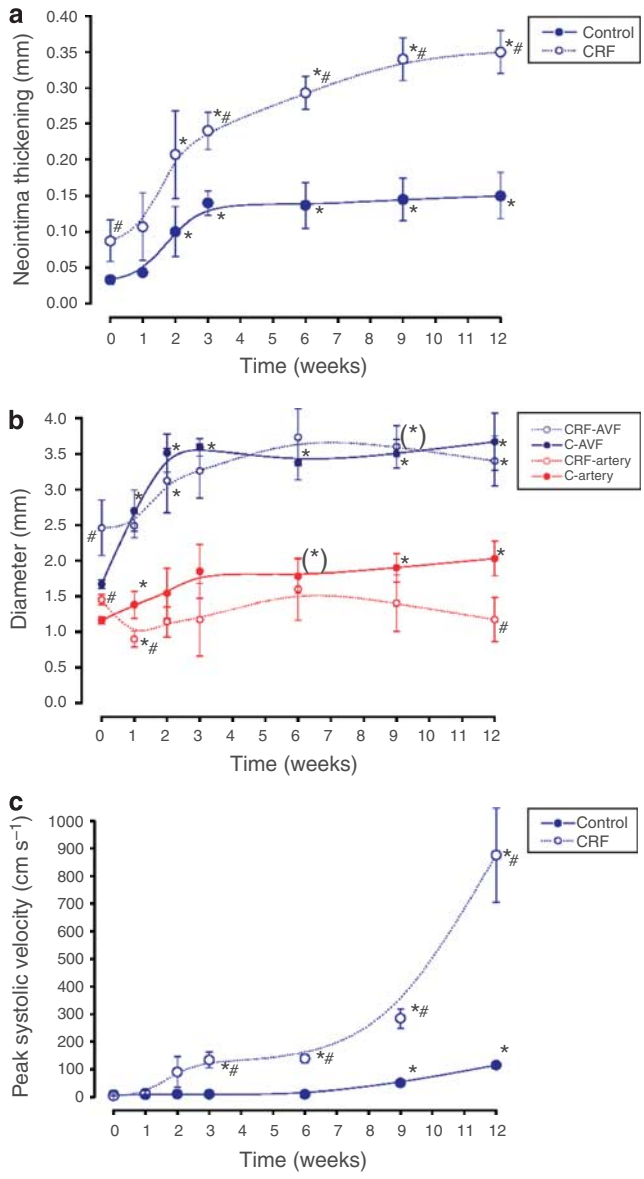

Figure 2 | Effects during a 12-week period of maturation. (**a**) Time course of neointimal thickening, (**b**) arterial and arteriovenous fistula (AVF) diameters, and (**c**) peak systolic velocity at the site of the anastomosis in chronic kidney disease (CKD) and control animals. $^{*}P < 0.05$ vs respective day 0, $^{\#}P < 0.05$ vs respective time point in the control group. C, control; CRF, chronic renal failure.

During fistula maturation, group no. 1 animals developed an increase in peak systolic velocity (baseline: 8 ± 4 cm/s, day 84: 115 ± 3 cm/s, $P = 0.02$), indicating a narrowing of the anastomosis. This was significantly pronounced in CKD animals (baseline: 3 ± 1 cm/s, day 84: 876 ± 171 cm/s, $P = 0.012$ vs baseline, $P = 0.008$ vs control at day 84) (Figure 2c). This increase in peak systolic velocity indicates that CKD animals are more prone to develop an AVF stenosis than controls.

Histomorphometric analysis of the neointima

For the histomorphometric analyses, hematoxylin and eosin-stained serial sections were used (Figure 3a–h). At baseline (control animals), the intima of femoral veins had a thickness of one to two cell layers (7.02 ± 2.16 µm). In contralateral femoral veins (day 84) of group no. 1 and group no. 2, the mean intima thickness was 6.61 ± 0.52 and 6.62 ± 0.53 µm, respectively (Figure 4a). Thus, neither modified contralateral hemodynamics nor chronic renal failure had an effect on nonarterialized veins. Figure 4b describes the progression of

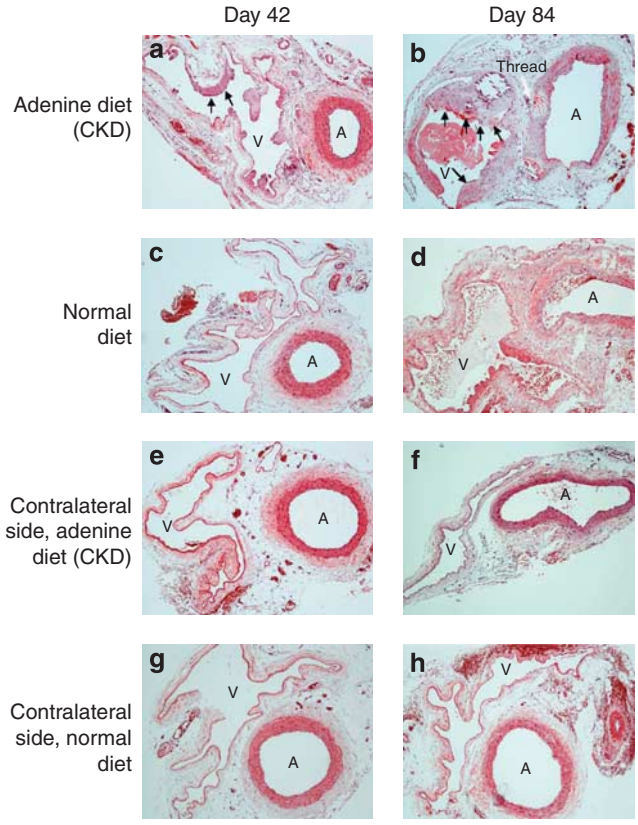

Figure 3 | Histological 2 µm cross sections stained with hematoxylin and eosin (× 100) of the arteriovenous fistula (AVF) anastomosis (level L3) and its respective contralateral vessels (femoral artery and vein). AVF on day 42 (**a**) and day 84 (**b**) in the chronic kidney disease (CKD) group. Note the extensive neointimal thickening (black arrow) in the fistula vein. White arrow shows surgical thread material. Significantly less neointimal hyperplasia in rats receiving normal diet (**c**, **d**). Intima and media of contralateral control vessels are not affected by the adenine diet (**e**, **f**) and have the same morphology as controls receiving normal diet (**g**, **h**). A, artery; V, vein.

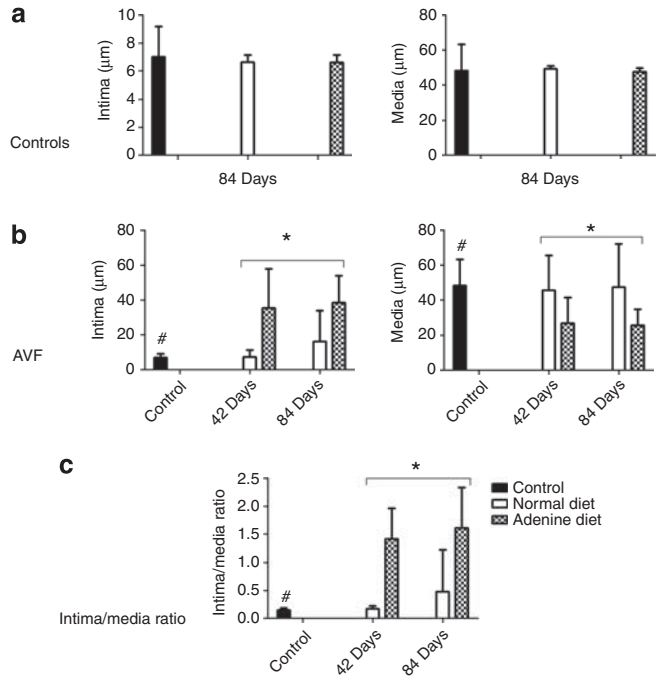

Figure 4 | Time course effect of chronic kidney disease (CKD) on neointimal thickening in the arteriovenous fistula (AVF). (**a**) Intima and media thickness of control femoral veins based on morphometry (average of level L1–L6). To exclude an effect of the diet and of contralateral hemodynamics, three different controls were performed: On day 84, femoral veins of rats without surgery (black bar), contralateral femoral veins of group no. 1 (white bar) and contralateral femoral veins of group no. 2 (shaded bar) animals had the same thickness, suggesting that neither the adenine diet nor the contralateral hemodynamics had systemic effects on neointimal development. (**b**) The intima increased significantly in chronic renal failure, days 42 and 84 after surgery. At the same time, the media decreased significantly. Consequently the intima/media ratio (**c**) showed a significant difference at day 42 and 84. $^{*}P<0.05$ vs respective day 0, $^{\#}P<0.05$ vs respective time point in group no. 2.

NIH after surgery in this model, based on morphometrical analysis. On days 42 and 84 after surgery, a marked neointimal thickening was observed in group no. 2, whereas in group no. 1 only a slight increase in neointima thickness developed as a consequence of the arterialized inflow. For both time points, this increase in NIH was significant ($P<0.014$). The changes in the media developed inversely, displayed by the media shrinking significantly in the CKD group, when compared with group no. 1 ($P<0.02$). Thus, intima/media thickness ratios showed a significant difference between both groups at both time points, too ($P<0.0002$) (Figure 4c). This indicates that maturation of arterialized veins in CKD was associated with a distinct growth of a neointimal complex accompanied with a diminution of the media. The thickness of the adventitial layer was nearly unaffected by the different diets throughout the study period.

Immunohistochemical staining

To characterize the cell composition within the neointima and the media, sections from level L3 were assessed, which represents the proximal side of the AVF anastomosis. Figure 5a–d describes the semiquantitative scores on days 42 and 84 after surgery. The majority of cells in both groups within the neointima were myofibroblasts. The images of Figure 5e–g show representative histological sections with NIH, demonstrating the abundance of myofibroblasts and the presence of SMCs. The data in Table 2 demonstrate that apoptosis and proliferation rates were significantly increased in group no. 2.

The dominant cell type within the media of the AVF in renal failure rats on days 42 and 84 after surgery was the myofibroblast too. On day 42, the media of group no. 1 rats showed significantly less vimentin-positive ($P<0.04$) and significantly more desmin-positive cells ($P<0.006$), indicating a higher amount of SMCs. On day 84, however, no significant difference in cellular phenotyping between both groups was revealed. Although the apoptosis rate showed no significant differences for both groups, the proliferation rate was significantly increased in the chronic renal failure group (Table 2).

Determination of AVF calcification

Analysis of von Kossa staining serial sections revealed significant calcification in animals of group no. 2 (Figure 6a and b; $P<0.0001$) when compared with group no. 1 (Figure 6c and d) and contralateral controls (Figure 6e–h). In healthy animals, just marginal calcification was observed at both the thread site and vein valves site. After 42 postoperative days, the arterial calcification in CKD animals was mostly located in the media of the afferent artery, suggesting a development of mediasclerosis. However, 84 days after surgery, calcification was found in both the intima and media layer. Here, a marked calcification of the fistula vein was also observed (Figure 6i). In particular, 83.3% of the intima and 61.1% of the media sections at levels L3–L6 representing the downstream vein, stained positive for calcification.

DISCUSSION

This is, to our knowledge, the first study that combines a detailed analysis of the structural changes in arterialized veins with a functional evaluation by means of noninvasive US imaging in small animals with CKD.

Our first major finding is that animals with CKD developed extensive NIH combined with a shrinking of the media layer, whereas healthy animals had only moderate neointimal formation as a response to the arterialized inflow. The second major finding is the severe calcification in fistula veins of CKD rats. Finally, the feeding artery and the fistula vein exhibit an inferior dilation after arterialization. Altogether, these adverse effects resulted in anastomotic stenoses with concomitant alterations of AVF hemodynamics.

Previous small animal studies were very useful in examining different pathomechanisms to analyze AVF failure.[7–11,13,14] None of these studies, however, had accurately depicted the clinical situation of patients with end-stage renal

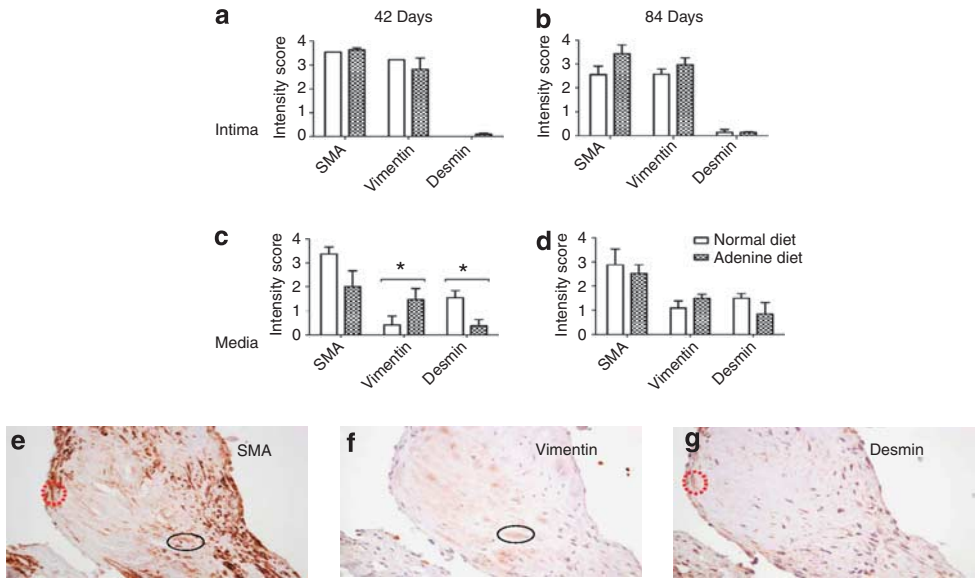

Figure 5 | Intensity scoring and cellular phenotyping in healthy and chronic kidney disease (CKD) rats. The cellular phenotype intensity score (positive cells for each of the specific marker as a percentage of the total number of cells; 0–10% = 0, 11–25% = 1, 26–50% = 2, 51–75% = 3, and 76–100% = 4) for the neointima (**a** and **b**) shows no difference in the cell composition within the intima between both groups. The intensity score for the media demonstrates significantly less vimentin-positive and significantly more desmin-positive cells in healthy animals on day 42 (**c**). In contrast, most of the cells within the shrunk media of CKD animals are myofibroblasts. On day 84, the media is primarily based on myofibroblasts in both groups (**d**). (**e**, **f**) Representative serial sections with extensive neointimal formation from level L3 stained for smooth muscle actin (SMA) (**e**), vimentin (**f**), and desmin (**g**). The predominant neointimal cell type is the SMA-positive and vimentin-positive myofibroblast (black lined ellipse). The red dotted ellipse shows an SMA-positive and desmin-positive contractile smooth muscle cell.

Table 2 | Histomorphometric analysis of apoptosis and proliferation within the intima and media on days 42 and 84 after surgery

	Postoperative day	Apoptosis (Tunel), %	Proliferation (PCN_1), %	A/P ratio
Intima				
Group no. 1	42	28 ± 10	32 ± 10	0.88
	84	21 ± 17	29 ± 11	0.72
Group no. 2 (CKD)	42	49 ± 17*	49 ± 6*	1.00
	84	42 ± 16*	40 ± 18*	1.05
Media				
Group no. 1	42	27 ± 16	12 ± 13	2.25
	84	41 ± 21	7 ± 7	5.85
Group no. 2 (CKD)	42	38 ± 12	31 ± 11*	1.23
	84	28 ± 17	15 ± 9*	1.87

Abbreviations: A/P ratio, **apoptosis/proliferation ratio;** CKD, chronic kidney disease.
*$P < 0.05$ vs respective group no. 1.
The values represent the percentage of positive cells for each of the specific markers as a percentage of the total number of cells. Rats of group no. 2 had a significant increased apoptosis and proliferation rate within the neointimal hyperplasia when compared with group no. 1. Regarding the media, more cells stained positive for apoptosis than proliferation in both groups; however, this effect was more distinguished in group no. 1.

disease, in which uremia may contribute to adverse vascular remodeling effects. To compensate for this, we successfully upgraded our previously described femoral AVF model[9] using rats with CKD induced by adenine.

There are several inherent advantages of our CKD model. Adenine-induced nephropathy is a well-established experimental model for the rat that strongly resembles the natural course of CKD in humans. This model is characterized by a gradual loss of renal function and presents many clinical features, which are associated with a chronic progressive renal failure.[15] It has been shown that the degree of uremia varies with dosage and length of the adenine administration and that the degree of uremia correlates with mortality. Therefore, we could induce a well-defined degree of CKD (serum levels of creatinine ranging from 48.5 to 80.5 mmol/l) that also allowed us to perform AVF surgery in these sick animals with acceptable mortality rates (<10%).

In contrast, a survival rate of only 33% is reported for the remnant kidney model 6 weeks after the surgical procedure.[16] This high mortality rate strongly limits the possibility of a longitudinal AVF maturation analysis, especially when the observation period has to be extended >6 weeks postoperatively. Furthermore, rats with remnant kidney are prone to develop hypertension, which may cause adverse hemodynamic effects.[17,18]

In our protocol, we have excluded a possible effect of systemic hypertension in CKD rats. Moreover, a direct effect of adenine on the vasculature was not detectable in contralateral femoral vessels. Therefore, we presumed that it was the uremic environment rather than indirect effects that caused the exacerbation of NIH and calcification within the AVFs. Our results confirmed that CKD induction using the adenine-enriched diet resulted in abnormal electrolyte metabolism, in particular, hypocalcemia and hyperphosphatemia and, furthermore, hypoalbuminemia and elevated serum creatinine values. This is in accordance with Yokozawa

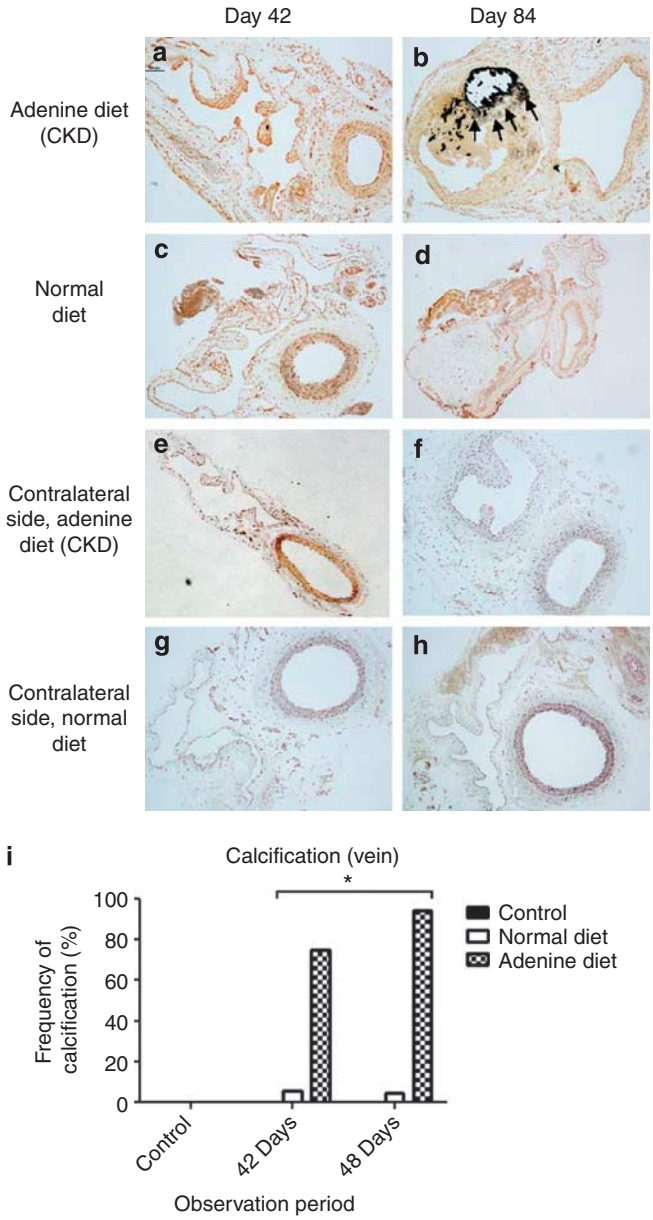

Figure 6 | Time course effect of chronic kidney disease (CKD) on vessel wall calcification in the fistula vein. An extensive calcification (black arrows) of the neointima and media were observed in CKD on days 42 (**a**) and 84 (**b**) after surgery. In contrast, the incidence of calcification in the downstream vein of group no. 1 was below 10% of the sections (**c** and **d**). No calcification occurred in control veins (**e**–**h**). The frequency of vein calcification was significantly increased in the CKD group (**i**), when compared with normal diet rats (*$P<0.05$ vs respective group no. 1).

et al.[15] and Katsumata *et al.*,[19] who proved close resemblance to metabolic abnormalities in human chronic renal failure.

Aggravation of NIH in animals with CKD

The NIH development in fistula veins is considered to be a multifactorial event.[3] There is increasing evidence that surgical trauma and modified hemodynamics are associated with endothelial and SMC damage.[20] In a few small[7,8,10,11] and large[21–25] animal studies, NIH formation could be repeatedly observed after AVF surgery and it has been shown that CKD accelerates NIH development.[12] To assess whether CKD resulted in specific morphological and functional changes, we have investigated AVFs noninvasively by means of US, and, combined these findings with histopathological analyses. In both experimental groups, we observed a development of NIH. Importantly, we show that the development of NIH was much more pronounced in CKD animals. In accordance with that observation, we found increased apoptosis- and proliferation-rates within the neointima, indicating an increased cell-turnover. This strongly suggests that metabolic abnormalities in CKD trigger adverse neointimal thickening in a short-term period after surgery. This, in fact, confirms the recent findings of Kokubo *et al.*,[12] who described an accelerated development of NIH within 3 weeks after surgery at the site of the anastomosis (jugular vein to carotid artery) in an experimental mouse model in animals with CKD. Extending these findings, we have determined that NIH developed not only within the anastomosis yet more downstream in the fistula vein, too. Moreover, we show that NIH development remained constant 21 days after surgery in healthy animals, but still continued in CKD animals until day 84 after AVF placement. A further novel observation is that, parallel to the NIH development, a significant shrinking of the media occurred in CKD rats. Because the proliferation rate within the media in these animals was significantly increased, we assume that the media substance loss in CKD was caused by an increased inward migration of SMC and myofibroblasts, which in turn confirms previous findings in patients.[26]

CKD causes neointimal and media calcification of fistula veins

It is well known that uremia-associated risk factors such as chronic inflammation and deficiencies of calcification inhibitors contribute to progressive vascular calcification in patients with end-stage renal disease.[27] The process does not merely consist in passive deposition of calcium phosphate crystals; it is clear that it is a well-organized process involving cell activity and specific protein synthesis.[28] Previous research concerning this matter focused exclusively on calcifying atherosclerosis of arteries,[5] and the role of calcification in veins has been marginally investigated so far.[6] In this study, we found marginal calcification in healthy animals at the site of the vein valves, which is in accordance to previous observations.[9] Nonetheless, the major novel finding is the significant calcification at all histological levels in animals with uremic background. Furthermore, this was accompanied with increased apoptosis levels within the neointima layer. Data from previous studies support a causal relationship between apoptotis and calcification.[29,30] Thus, our results suggest that calcification in fistula veins is aggravated by a CKD-induced SMC apoptosis.

It has been recently shown that arterial vessel calcification in dialysis patients was associated with a large extent of undercarboxylated matrix-Gla protein expression, which indicates an exhaustion of local calcification inhibition capability.[31] In contrast to the typical media-sclerosis in arteries, we have found both a rapid development of neointimal and media calcification located at the site of the anastomosis and within the wall of the fistula vein. This suggests that the surgical trauma and the foreign suture material may influence the deposition of the calcium. However, we can exclude this effect in the downstream fistula vein, in which the calcification was almost the same. Taken together, an important impairment of local calcification inhibitors in CKD can be assumed and further investigation is essential.

Impaired AVF maturation

In patients, vein dilation after arterialization is a part of a physiological AVF maturation process, which makes recurrent cannulation for dialysis possible. In general, a change of hemodynamic parameters—increase of blood pressure, flow volume, and wall shear stress—causes a physiological dilation in the downstream vein. This response returns shear-stress levels back toward their baseline.[3] In the setting of early AVF failure, the role of insufficient dilation is unclear, but it is well known that fistula vein dilatation occurs rapidly after AVF creation.[32,33] Accordingly, we have observed an $\sim$220% increase in fistula vein diameter in healthy animals within 6 weeks, whereby this dilation remained stable thereafter. In contrast, CKD was associated with an impairment of fistula vein dilation after surgery. Moreover, the afferent artery is also adversely affected. This implies that CKD adversely affects the ability of the vessels to dilate, which is consequently an adverse effect for the maturation process. Our data strongly suggest that the impaired dilation of fistula veins in CKD is a result of the extended calcification as well as the significant increase of myofibroblasts, which represent the major source for extracellular collagen deposition within the vein wall. It has also been reported that the predominant cell type within NIH formation is the myofibroblast in patients with end-stage renal disease.[34] Thus, our rat model offers an excellent experimental setting to test future novel therapies that will target myofibroblast function.

Development of AVF stenosis

In our study, aggravation of neointimal thickening, progressive access calcification, and impaired dilation all lead to increased flow velocities in the US investigations that indicate a reduction of luminal area and, ultimately, a development of AVF stenosis. In an experimental porcine AVF model, Misra *et al.*[22] showed increased shear-stress levels at the site of vein-to-graft anastomosis on days 1, 3, and 7 after surgery. We assume that CKD may potentiate those adverse biomechanical forces at the site of high-flow velocity regions in fistula veins; this, in turn, is a vicious cycle that aggravates NIH development.

Our data illustrate that CKD itself triggers adverse effects in AVFs. This leads to impaired vascular remodeling contributing to AVF stenosis. Consequently, AVF surgery in adenine-induced renal failure rats provides the research community a reliable model that can be used to test novel therapeutic strategies to improve AVF maturation and patency in hemodialysis patients.

MATERIALS AND METHODS

Female 12-week-old Sprague–Dawley rats (270–330 g) were purchased from a commercial breeder (Charles River Wiga GmbH, Sulzfeld, Germany). They were kept in a climate-controlled room (21 °C and 60% relative humidity) with a 12-h cycle of light and darkness and were housed in normal cages with free access to water and food. All experiments were approved by the local animal human board and were performed in accordance with the legislation on the protection of animals (AZ 50.203.2-AC 26, 54/06).

Adenine diet-induced CKD

It has been shown that a long-term feeding of adenine to rats produces metabolic abnormalities resembling chronic renal failure in humans.[15,35] This feeding of adenine to rats results in interstitial nephritis, in particular in the deposition of 2,8-dihydroxyadenine in the renal tubules, which subsequently induces a degeneration, interstitial fibrosis, and atrophy of the proximal and distal tubules,[19] leading to the accumulation of various guanidine compounds and urea nitrogen in the blood.

Experimental groups

A total of 28 animals was used for this study. Twenty-four rats were separated into two groups ($n = 12$ rats/group); four animals served as healthy controls. The rats of group no. 1 along with the four healthy controls received commercial feed, whereas the animals of group no. 2 received an adenine-rich diet (0.75% adenine, ssniff Spezialdiäten GmbH, Soest, Germany) preoperatively for 3 weeks to induce CKD. The level of renal insufficiency was controlled using serum creatinine values. When CKD was established in group no. 2, both groups underwent AVF surgery. Due to decreasing serum creatinine levels 6 weeks postoperatively, the animals of group no. 2 were again fed with adenine-enriched diet for 1 week. The AVF rats of both groups were postoperatively examined with high-resolution US on days 1, 7, 14, 21, 42, 63, and 84. As shown in Figure 7, half of the animals of each group was killed and their tissues were harvested on days 42 and 84, respectively.

Microsurgical procedure

Animals underwent AVF surgery on the right femoral artery as previously described.[9] Briefly, the femoral vein was anastomosed to the femoral artery in an end-to-side manner using a 10–0 monofilament (Serapren, Serag-Wiessner, Naila, Germany) running suture. A dilation of the arterialized vein could be observed shortly after clamp removal (Figure 8a).

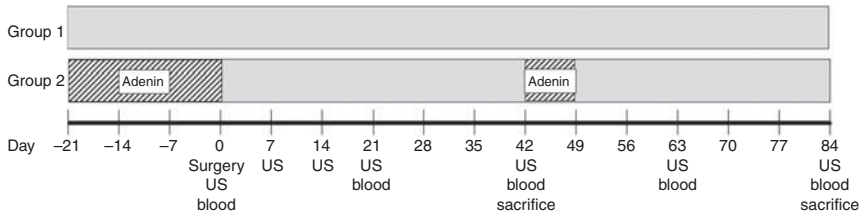

Figure 7 | The study design shows a total study period of 15 weeks. Of these, 3 weeks were the preoperative time, when rats of the chronic kidney disease group (group 2) received an adenine-rich diet. Because of decreasing serum creatinine values after 42 postoperative days, animals of group 2 again received an adenine-rich diet for 1 week. On day 0, rats underwent arteriovenous fistula (AVF) surgery. Ultrasound investigations were performed periodically during the 12 postoperative weeks. Rats were killed on days 42 (week 6) and 84 (week 12) after surgery.

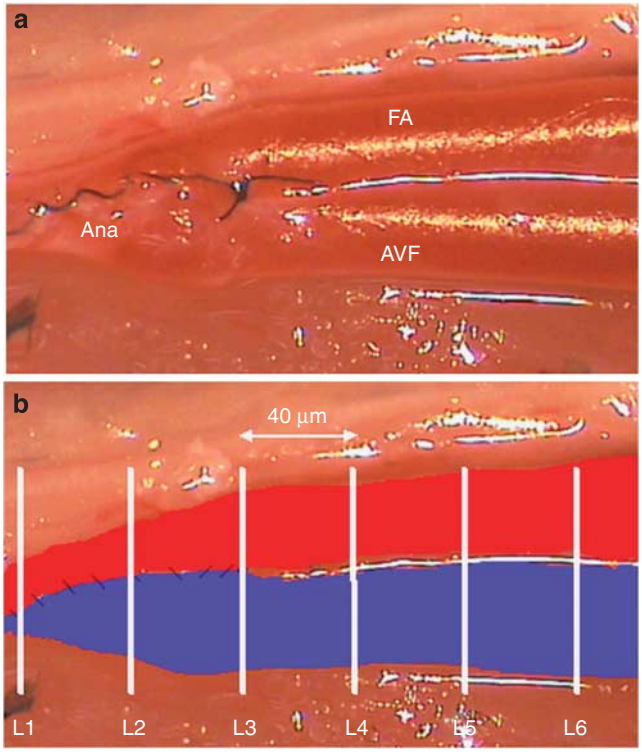

Figure 8 | AVF of the end of the surgical procedure after clamp removal. (**a**) Intraoperative image (25-fold magnification). The running suture shows the site of the end-to-side anastomosis (Ana) between the femoral artery (FA) and femoral vein, resulting in an arteriovenous fistula (AVF). (**b**) Schematic illustration of the histological section levels (L1–L6). L1 is at the distal side of the anastomosis; L2 is at the middle part where the diameter of both participating artery and vein are of equal size; L3 is at the proximal side of the anastomosis. The next three levels are lined every 40 µm, meaning every 20 serial sections of 2 µm thickness (L4, L5, and L6, respectively).

Table 3 | List of antibodies and negative controls that were used for the immunohistological staining

Antibody			Negative control	
	Company	Dilution		Company
α-Smooth muscle actin	DAKO M0851	1:300	IgG2a	DAKO X0943
Vimentin	DAKO M0725	1:100	IgG1	DAKO X0931
Desmin	DAKO M0760	1:100	IgG1	DAKO X0931
PCNA	DAKO M0879	1:400	IgG2a	DAKO X0943

Abbreviations: IgG, immunoglobulin G; PCNA, proliferating-cell nuclear antigen.

High-resolution US

The afferent femoral artery, anastomosis, and fistula vein were visualized with a 12-MHz transducer (GE Vivid pro 7, GE Medical Systems, Solingen, Germany). After the characteristic blood flow pattern of the vessel was identified, the position of the probe was optimized to show clear vessel wall/lumen interfaces and longitudinal B-Mode images. Moreover, Doppler signals were recorded. Vessel diameters and neointimal thickness were measured by automated analysis software (Brachial Analyzer, Medical Imaging Applications, Iowa City, IO, USA).

Measurement of systolic blood pressure

Systolic blood pressure was measured using the tail-cuff method (Softron BP-98A, Softron; Tokio, Japan). Rats were put in a restriction cage that was placed in a 37 °C heated tube for 15 min. The cuff that occluded the flow of blood into the tail was inflated to a maximum of 200 mm Hg and deflated automatically at a rate of 10 mm Hg/s. Animals were habituated to the procedure by 10 cycles of inflation and deflation. Thereafter, six measurements were performed with each animal, and mean values were calculated.

Harvesting, specimen preparation, and terminology

Tissue harvesting was performed as previously described.[9] The entire AVF was removed *en bloc* and placed in formaline, embedded in paraffin, and serially sectioned in 2 µm sections. The AVF anastomosis and downstream fistula vein were longitudinally divided into six parts as depicted in Figure 8b. Histological sections from each proceeded for evaluation.

Histological and immunohistochemical analysis

Sections from each level were stained with hematoxylin and eosin, elastica van Gieson, and von Kossa. Immunohistology was performed using commercial antibodies (Table 3). Standard immunohistochemistry protocols were followed; deparafinization and hydration was followed by antigen demasking (2% cintate buffer in a microwave) and nonspecific protein binding with 1% fetal calf serum in Tris buffer for 10 min, Avidin D solution for 10 min and Biotin solution for 10 min (Vector Kit SP 2001, Vector Laboratories, Burlingame, UK). Primary antibody incubation took place

overnight at 4 °C and a secondary antibody blend incubation followed for 10 min at room temperature, followed with streptavidin/horseradish peroxidase incubation for 10 min (DAKO-Kit LSAB2 System-HRP K0673, DAKO, Hamburg, Germany). Substrate solution was applied for development (NovaRED, Vector SK-4800, Vector Laboratories) and counterstaining with hematoxylin.

A TdT-mediated dUTP nick end labeling reaction was performed according to the manufacturer's instructions (*In situ* Cell Death detection kit, POD, Roche 11684817910, Roche Diagnostics GmbH/Roche Applied Science, Mannheim, Germany) for the assessment of apoptosis in serial sections to the ones stained with proliferating-cell nuclear antigen for proliferation.

Histomorphometric analysis and identification of cellular phenotypes

Two sections from each level (L1 to L6, Figure 2b) were sampled in order to measure their respective intima-, media-, and adventitia thickness. Twenty equidistant radial measurements were conducted for each layer, and the values were averaged. Histographs from hematoxylin and eosin- and elastica van Gieson-stained sections were taken at a final magnification of $\times 40$ using a Nikon Eclipse 80i microscope, a Nikon Digital sight DS-2 Mv camera (Nikon GmbH, Duesseldorf, Germany) and a Windows work station. Nikon NIS-Elements D 3.0 software was used for morphometric analyses.

To evaluate calcification, sections from every level were stained with von Kossa stain. These stains were scored as positive or negative depending on whether calcium crystals were observed or not. For each level, the presence of theses crystals was scored and the location documented (Vessel, layer, suture).

Different combinations of immunohistological stains on serial sections were used to differentiate between

- contractile medial-like SMCs (smooth muscle actin (SMA) positive, vimentin negative, desmin positive),
- myofibroblasts (smooth muscle actin positive, vimentin positive, desmin negative) and
- fibroblasts (smooth muscle actin negative, vimentin positive, desmin negative).
- As previously introduced by Chaudhury *et al.*,[34] a semiquantitative intensity scoring scale from 0 to 4 was used to quantify the percentage of positive cells for the specific markers.

Blood biochemistry

Serum phosphorous, serum calcium, and serum creatinine levels were determined using an autoanalyzer (Vitros 250, Ortho-Clinical Diagnostics, Strassbourg, France).

Statistics

Continuous data were reported as arithmetic mean ± s.d.; categorical data were expressed as frequencies and percentage. The primary test for an effect inferred from US-generated data was a test of the interaction in a one-way repeated measures analysis of variance. The family of pairwise comparisons was conducted using the Holm-Sidak method.

The histomorphometric data were analyzed using a repeated measures analysis of variance model taking into account the multiple measurements per animal from different intersectional planes. The median of the 20 measurements per layer was used in order to reduce variability in the data due to artefacts. Calcification frequencies were compared using Fisher's exact test.

P-Values <0.05 were considered as significant. All analyses were performed with SigmaStat 3.5 (Systat Software, San Jose, CA, USA) or SAS 9.1 (Copyright © 2002–2003 by SAS Institute, Cary, NC, USA.).

DISCLOSURE

All the authors declared no competing interests.

ACKNOWLEDGMENTS

The study was funded by the research promotion program 'START' of the medical faculty of the RWTH Aachen University, Germany (Title: 'Die Arterialisation venöser Gefäße').

REFERENCES

1. Tordoir J, Canaud B, Haage P *et al.* EBPG on vascular access. *Nephrol Dial Transplant* 2007; **22**(Suppl 2): ii88–ii117.
2. Biuckians A, Scott EC, Meier GH *et al.* The natural history of autologous fistulas as first-time dialysis access in the KDOQI era. *J Vasc Surg* 2008; **47**: 415–421.
3. Roy-Chaudhury P, Spergel LM, Besarab A *et al.* Biology of arteriovenous fistula failure. *J Nephrol* 2007; **20**: 150–163.
4. Murphy GJ, Saunders R, Metcalfe M *et al.* Elbow fistulas using autogeneous vein: patency rates and results of revision. *Postgrad Med J* 2002; **78**: 483–486.
5. Floege J, Ketteler M. Vascular calcification in patients with end-stage renal disease. *Nephrol Dial Transplant* 2004; **19**(Suppl 5): V59–V66.
6. Schlieper G, Kruger T, Djuric Z *et al.* Vascular access calcification predicts mortality in hemodialysis patients. *Kidney Int* 2008; **74**: 1582–1587.
7. Castier Y, Lehoux S, Hu Y *et al.* Characterization of neointima lesions associated with arteriovenous fistulas in a mouse model. *Kidney Int* 2006; **70**: 315–320.
8. Chan CY, Chen YS, Ma MC *et al.* Remodeling of experimental arteriovenous fistula with increased matrix metalloproteinase expression in rats. *J Vasc Surg* 2007; **45**: 804–811.
9. Langer S, Heiss C, Paulus N *et al.* Functional and structural response of arterialized femoral veins in a rodent AV fistula model. *Nephrol Dial Transplant* 2009; **24**: 2201–2206.
10. Lin T, Horsfield C, Robson MG. Arteriovenous fistula in the rat tail: a new model of hemodialysis access dysfunction. *Kidney Int* 2008; **74**: 528–531.
11. Misra S, Fu AA, Anderson JL *et al.* The rat femoral arteriovenous fistula model: increased expression of matrix metalloproteinase-2 and -9 at the venous stenosis. *J Vasc Interv Radiol* 2008; **19**: 587–594.
12. Kokubo T, Ishikawa N, Uchida H *et al.* CKD accelerates development of neointimal hyperplasia in arteriovenous fistulas. *J Am Soc Nephrol* 2009; **20**: 1236–1245.
13. Abbruzzese TA, Guzman RJ, Martin RL *et al.* Matrix metalloproteinase inhibition limits arterial enlargements in a rodent arteriovenous fistula model. *Surgery* 1998; **124**: 328–334.
14. Caplice NM, Wang S, Tracz M *et al.* Neoangiogenesis and the presence of progenitor cells in the venous limb of an arteriovenous fistula in the rat. *Am J Physiol Renal Physiol* 2007; **293**: F470–F475.
15. Yokozawa T, Zheng PD, Oura H *et al.* Animal model of adenine-induced chronic renal failure in rats. *Nephron* 1986; **44**: 230–234.
16. Bahlmann FH, Song R, Boehm SM *et al.* Low-dose therapy with the long-acting erythropoietin analogue darbepoetin alpha persistently activates endothelial Akt and attenuates progressive organ failure. *Circulation* 2004; **110**: 1006–1012.

17. Matsuguma K, Ueda S, Yamagishi S *et al.* Molecular mechanism for elevation of asymmetric dimethylarginine and its role for hypertension in chronic kidney disease. *J Am Soc Nephrol* 2006; **17**: 2176–2183.
18. Croatt AJ, Grande JP, Hernandez MC *et al.* Characterization of a model of an arteriovenous fistula in the rat. The effect of L-NAME. *Am J Pathol* 2010; **176**: 2530–2541.
19. Katsumata K, Kusano K, Hirata M *et al.* Sevelamer hydrochloride prevents ectopic calcification and renal osteodystrophy in chronic renal failure rats. *Kidney Int* 2003; **64**: 441–450.
20. Roy-Chaudhury P, Sukhatme VP, Cheung AK. Hemodialysis vascular access dysfunction: a cellular and molecular viewpoint. *J Am Soc Nephrol* 2006; **17**: 1112–1127.
21. Dobrin PB, Littooy FN, Golan J *et al.* Mechanical and histologic changes in canine vein grafts. *J Surg Res* 1988; **44**: 259–265.
22. Misra S, Woodrum DA, Homburger J *et al.* Assessment of wall shear stress changes in arteries and veins of arteriovenous polytetrafluoroethylene grafts using magnetic resonance imaging. *Cardiovasc Intervent Radiol* 2006; **29**: 624–629.
23. Misra S, Fu AA, Anderson JL *et al.* Fetuin-A expression in early venous stenosis formation in a porcine model of hemodialysis graft failure. *J Vasc Interv Radiol* 2008; **19**: 1477–1482.
24. Misra S, Fu AA, Puggioni A *et al.* Increased shear stress with upregulation of VEGF-A and its receptors and MMP-2, MMP-9, and TIMP-1 in venous stenosis of hemodialysis grafts. *Am J Physiol Heart Circ Physiol* 2008; **294**: H2219–H2230.
25. Wang Y, Krishnamoorthy M, Banerjee R *et al.* Venous stenosis in a pig arteriovenous fistula model–anatomy, mechanisms and cellular phenotypes. *Nephrol Dial Transplant* 2008; **23**: 525–533.
26. Roy-Chaudhury P, Arend L, Zhang J *et al.* Neointimal hyperplasia in early arteriovenous fistula failure. *Am J Kidney Dis* 2007; **50**: 782–790.
27. Ketteler M, Schlieper G, Floege J. Calcification and cardiovascular health: new insights into an old phenomenon. *Hypertension* 2006; **47**: 1027–1034.
28. Cozzolino M, Dusso AS, Slatopolsky E. Role of calcium-phosphate product and bone-associated proteins on vascular calcification in renal failure. *J Am Soc Nephrol* 2001; **12**: 2511–2516.
29. Clarke MC, Littlewood TD, Figg N *et al.* Chronic apoptosis of vascular smooth muscle cells accelerates atherosclerosis and promotes calcification and medial degeneration. *Circ Res* 2008; **102**: 1529–1538.
30. Shroff RC, McNair R, Skepper JN *et al.* Chronic mineral dysregulation promotes vascular smooth muscle cell adaptation and extracellular matrix calcification. *J Am Soc Nephrol* 2009; **21**: 103–112.
31. Shroff RC, McNair R, Figg N *et al.* Dialysis accelerates medial vascular calcification in part by triggering smooth muscle cell apoptosis. *Circulation* 2008; **118**: 1748–1757.
32. Corpataux JM, Haesler E, Silacci P *et al.* Low-pressure environment and remodelling of the forearm vein in Brescia-Cimino haemodialysis access. *Nephrol Dial Transplant* 2002; **17**: 1057–1062.
33. Wong V, Ward R, Taylor J *et al.* Factors associated with early failure of arteriovenous fistulae for haemodialysis access. *Eur J Vasc Endovasc Surg* 1996; **12**: 207–213.
34. Roy-Chaudhury P, Wang Y, Krishnamoorthy M *et al.* Cellular phenotypes in human stenotic lesions from haemodialysis vascular access. *Nephrol Dial Transplant* 2009; **24**: 2786–2791.
35. Neven E, Dams G, Postnov A *et al.* Adequate phosphate binding with lanthanum carbonate attenuates arterial calcification in chronic renal failure rats. *Nephrol Dial Transplant* 2009; **24**: 1790–1799.